FACTA UNIVERSITATIS
Series: **Mechanical Engineering**
https://doi.org/10.22190/FUME230125009B

Original scientific paper

DISCRETE-TIME MODEL-BASED SLIDING MODE CONTROLLERS FOR TOWER CRANE SYSTEMS

Anamaria-Ioana Borlea[1], Radu-Emil Precup[1,2], Raul-Cristian Roman[1]

[1]Politehnica University of Timisoara, Department of Automation and Applied Informatics, Timisoara, Romania
[2]Romanian Academy – Timisoara Branch, Center for Fundamental and Advanced Technical Research, Timisoara, Romania

Abstract. *This paper applies three classical and very popular discrete-time model-based sliding mode controllers, namely the Furuta controller, the Gao controller, and the quasi-relay controller due to Milosavljević, to the position control of tower crane systems. Three single input-single output (SISO) control systems are considered, for cart position control, arm angular position control and payload position control, and separate SISO controllers are designed in each control system. Experimental results are included to support the comparison of the three plus three plus three sliding mode controllers.*

Key words: *Discrete-time model-based sliding mode controllers, Furuta controller, Gao controller, Tower crane systems*

1. INTRODUCTION

Sliding Mode Control (SMC) is a particular kind of variable structure system originated in the early 60's [1]. The main idea of the general Variable Structure Control (VSC) laws is to use a high-speed switching control scheme to drive the process state trajectory onto a specified hyper-surface, which is commonly called the sliding surface or switching surface, and next keep the process state trajectory moving along this surface [2] in order to meet the performance specifications imposed to the control system.

Received: January 25, 2023 / Accepted March 05, 2023
Corresponding author: Radu-Emil Precup
Politehnica University of Timisoara, Department of Automation and Applied Informatics, Bd. V. Parvan 2, 300223 Timisoara, Romania
Romanian Academy – Timisoara Branch, Center for Fundamental and Advanced Technical Research, Bd. Mihai Viteazu 24, 300223 Timisoara, Romania
E-mail: radu.precup@aut.upt.ro

The discontinuous nature of the control signal helps to maintain a high performance of SMC and VSC by switching between two distinct control structures [3]. Because of this switching behavior, SMC can have some dead zones for parameters variations, and is not sensitive to disturbances [4].

This paper is focused on SMC of tower crane systems. Such control approaches are outlined as follows. In [5], a continuous-time SMC law is designed based on a nonlinear model of a Tower Crane System (TCS). Two variants of discrete-time data-driven SMC laws for TCSs are presented in [6].

Many papers on different controllers for cranes have been reported in the past years. The SMC problem for overhead crane is the subject of [7], which describes a model based integral SMC scheme for discrete-time systems. The authors of [8] offer a model-based combination of SMC. Second-order SMC for controlling the trolley in the XOY plane is addressed in [9]. An adaptive fuzzy SMC is developed by [10] for trolley position and sway control in the XOY plane, where two linear sliding surfaces are defined for the position and sway angle.

Tower cranes can be found in fewer papers then overhead cranes because of their increased complexity. An adaptive control scheme for underactuated tower cranes is proposed in [11] to achieve simultaneous slew/translation positioning and swing suppression, using this approach is no need for linearize the tower crane dynamical equations around the equilibrium point or to neglect nonlinear terms. Controllers which are composed of partial feedback linearization and SMC are suggested in [13], guaranteeing the robustness in the case of variations of several system parameters. Integral Sliding Mode Control (ISMC) for tower cranes is proposed in [13] to ensure precise tracking of the desired position while reducing the oscillations of the payload. The controller in [13] is designed using a high fidelity nonlinear dynamical model, however, the switching gain must be limited to implement the SMC on the real TCS, and as a result a steady-state error will be present in the system's outputs; this shortcoming is overcome using ISMC.

The purpose of this paper is to apply model-based SMC to a representative nonlinear process, namely the TCS. To demonstrate the performance of these approaches, the validation through experiments is presented. Three approaches to Discrete Time Sliding Mode Control (DTSMC) are described based on the mathematical model of the process: the DTSMC law in the approach proposed by K. Furuta [14], the DTSMC law in the approach proposed by W.-B. Gao et al. [15] and the DTSMC law of quasi-relay type proposed by Č. Milosavljević [16].

The remainder of this paper is organized as follows. In Section 2, the DTSMC problem formulation and the three control laws are described. The validation study is presented in Section 3. Conclusions are presented in Section 4.

2. MODEL-BASED SLIDING MODE CONTROL PROBLEM FORMULATION

Let the dynamical discrete-time system be described by the following single input linear time-invariant state-space mathematical model:

$$P:\begin{cases}\mathbf{x}_{k+1}=\mathbf{A}\cdot\mathbf{x}_k+\mathbf{B}\cdot u_k,\\ \mathbf{y}_k=\mathbf{C}\cdot\mathbf{x}_k,\end{cases} \tag{1}$$

where $\mathbf{x}_k = [x_{k,1} \ \dots \ x_{k,n}]^T \in \Re^n$ is the state vector, T indicates matrix transposition, k indicates the discrete time (sampling interval) index, $k \in Z$, $k \geq 0$, the (scalar) control input is $u_k \in \Re$, $\mathbf{y}_k = [y_{k,1} \ \dots \ y_{k,p}]^T \in \Re^p$ is the output vector, and $\mathbf{A} \in \Re^{n \times n}$, $\mathbf{B} \in \Re^{n \times 1}$ and $\mathbf{C} \in \Re^{p \times n}$ are the system matrix, the input matrix, the output matrix, respectively [17]. Although the model in (1) is linear, the aim of SMC is to control nonlinear processes; however, this linear model is considered as it allows a relatively simple analysis and design of the control systems according to [14], [15] and [16].

Using the notation s_k for the switching variable, the sliding hyper-surface

$$S = \{\mathbf{x}_k \in \Re^n \,|\, s_k = \mathbf{K}\cdot\mathbf{x}_k = 0\} \subset \Re^n \tag{2}$$

is determined by choosing the gain matrix of the sliding hyper-surface $\mathbf{K} \in \Re^{1 \times n}$ so that the system (1) is stable as long as $\mathbf{x}_k$ remains on S [14].

2.1 Furuta DTSMC law

A type of DTSMC system is proposed by K. Furuta in [14], in which the discrete-time control law for the system (1), referred to here as the Furuta DTSMC law, is

$$u_k = u_k^{eq} + u_k^d, \tag{3}$$

where u_k^d is discontinuous control input and the equivalent control input is u_k^{eq}. Imposing $\Delta s_k = 0$, the control law to keep the state on (2) is given by

$$\begin{aligned} u_k^{eq} &= \mathbf{F}_{eq}\cdot\mathbf{x}_k,\\ \mathbf{F}_{eq} &= -(\mathbf{K}\cdot\mathbf{B})^{-1}\cdot\mathbf{K}\cdot(\mathbf{A}-\mathbf{I}) \in \Re^{1\times n}, \end{aligned} \tag{4}$$

with $\mathbf{I}$ – the identity matrix of order n.

The discontinuous control law is described as

$$\begin{aligned} u_k^d &= \mathbf{F}_d\cdot\mathbf{x}_k,\\ \mathbf{F}_d &= [f_1 \ \dots \ f_n]^T \in \Re^{1\times n}. \end{aligned} \tag{5}$$

It is proved in [14] that the system (1) controlled with the control law in (3) is stable if the absolute value of the i^{th} element of $\mathbf{F}_d$, i.e. f_i, $i=1\dots n$, satisfies

$$f_i = \begin{cases} f_0 & \text{if} \quad (\mathbf{K}\cdot\mathbf{B})\cdot s_k\cdot x_{k,i} < -\delta_i,\\ 0 & \text{if} \quad |(\mathbf{K}\cdot\mathbf{B})\cdot s_k\cdot x_{k,i}| \leq \delta_i,\\ -f_0 & \text{if} \quad (\mathbf{K}\cdot\mathbf{B})\cdot s_k\cdot x_{k,i} > \delta_i, \end{cases} \tag{6}$$

in which $x_{k,i}$ is the i^{th} element of $\mathbf{x}_k$ and δ_i is defined as

$$\delta_i = 0.5\cdot f_0\cdot|x_{k,i}|\cdot(\mathbf{K}\cdot\mathbf{B})^2\cdot\sum_{j=1}^{n}|x_{k,j}|, \tag{7}$$

with the amplitude of f_0 limited by

$$0 < f_0 < \frac{2}{\left|(\mathbf{K}\cdot\mathbf{B})\sum_{j=1}^{n} t_{1j}\right|}, \tag{8}$$

where $\mathbf{t}_1$ is the first column of the matrix $[\mathbf{t}_1\ \mathbf{t}_2\ \ldots\ \mathbf{t}_n]$ in which t_{1i} is the i^{th} element of $\mathbf{t}_1$ satisfying $\mathbf{K}\cdot\mathbf{t}_1=1$, $\mathbf{K}\cdot\mathbf{t}_i=1$, $i=2\ldots n$; furthermore $\mathbf{t}_1$ and $\mathbf{t}_i$, with $i=2\ldots n$, are linearly independent [14].

The gain matrix $\mathbf{K}$ shall be designed so that the system [14]

$$\mathbf{x}_{k+1} = [\mathbf{A} - \mathbf{B}\cdot(\mathbf{K}\cdot\mathbf{B})^{-1}\cdot\mathbf{K}\cdot(\mathbf{A}-\mathbf{I})]\cdot\mathbf{x}_k \tag{9}$$

is stable. The performance specifications imposed to the control system are zero stationary control with respect to constant reference inputs and reasonable settling time. The guidelines to design the Furuta DTSMC law such that to meet these performance specifications will be given in Section 3.1.

2.2 Gao DTSMC law

A type of SMC system is described by W.-B. Gao et al. in [15], where the dynamic behavior of the reaching law is as follows:

$$s_{k+1} - s_k = -q\cdot T_s\cdot s_k - \varepsilon\cdot T_s\cdot \operatorname{sgn}(s_k), \tag{10}$$

where T_s is the sampling period, q is a scalar parameter that fulfills $q\cdot T_s\in(0,1)$ and $\varepsilon>0$ is a parameter.

Solving for u_k the equation obtained from (1), (2) and (10) leads to the following control law, referred to here as the Gao DTSMC law [15]:

$$u_k = -\frac{1}{(\mathbf{K}\cdot\mathbf{B})}\cdot\{\mathbf{K}\cdot[\mathbf{A}-(1-q\cdot T_s)\cdot\mathbf{I}]\cdot\mathbf{x}_k + \varepsilon\cdot T_s\cdot\operatorname{sgn}(\mathbf{K}\cdot\mathbf{x}_k)\}. \tag{11}$$

Imposing the same performance specifications as in Section 3.1, the guidelines to design the Gao DTSMC law will be presented in Section 3.2.

2.3 Quasi-relay DTSMC law

Č. Milosavljević describes in detail in [16] the quasi-relay control law for the system (1), referred to as the quasi-relay DTSMC law, with the expression

$$u_k = -\left(\sum_{i=1}^{r}\omega_i\left|x_{k,i}\right|\right)\operatorname{sgn}(s_k), r\le n-1, \tag{12}$$

where $\omega_i>1$ are the parameters which must be chosen by the designer.

The general condition of existence and achievement of the quasi-sliding mode is [16]

$$|s_{k+1}|<|s_k|,\ k\in\mathrm{Z}, k\ge 0. \tag{13}$$

Imposing the same performance specifications as in Section 3.1, the guidelines to design the quasi-relay DTSMC law will be specified in Section 3.3.

3. VALIDATION CASE STUDY

The TCS is presented in detail in [6] and [18], as representative process to validate various controls algorithms including those discussed in relation with this process. The TCS is a nonlinear electromechanical system with a complex dynamic behavior. The system illustrated in Fig. 1 has three controlled outputs, namely the cart position y_1(m)=x_3(m), the arm angular position y_2(rad)=x_4(rad) and the payload position y_3(m)=x_9(m).

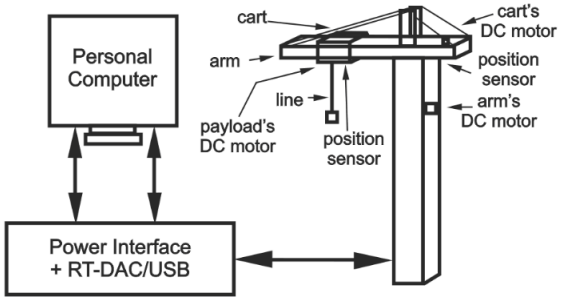

Fig. 1 Block diagram of principle of Tower Crane system [6].

The three actuators shown in Fig. 1 are Direct Current (DC) motors, and Pulse Width Modulation (PWM) is involved. The variable $m_1 \in [-1, 1]$ is the output of the saturation and dead zone static nonlinearity specific to the first actuator:

$$m_1(t) = \begin{cases} -1, & \text{if } u_1(t) \le -u_{b1}, \\ (u_1(t)+u_{c1})/(u_{b1}-u_{c1}), & \text{if } -u_{b1} < u_1(t) < -u_{c1}, \\ 0, & \text{if } -u_{c1} \le \lvert u_1(t) \rvert \le u_{a1}, \\ (u_1(t)-u_{a1})/(u_{b1}-u_{a1}), & \text{if } u_{a1} < u_1(t) < u_{b1}, \\ 1, & \text{if } u_1(t) \ge u_{b1}, \end{cases} \tag{14}$$

where t is the continuous time argument, $t \in \Re$, $t \ge 0$, $u_1(\%) \in [-100, 100]$ and $u_1 \in [-1, 1]$ is the first control input for cart position control, and the values of the parameters in (14) are [6] u_{a1}=0.1925, u_{b1}=1 and u_{c1}=0.2. The variable $m_2 \in [-1, 1]$ is the output of the saturation and dead zone static nonlinearity specific to the second actuator:

$$m_2(t) = \begin{cases} -1, & \text{if } u_2(t) \le -u_{b2}, \\ (u_2(t)+u_{c2})/(u_{b2}-u_{c2}), & \text{if } -u_{b2} < u_2(t) < -u_{c2}, \\ 0, & \text{if } -u_{c2} \le \lvert u_2(t) \rvert \le u_{a2}, \\ (u_2(t)-u_{a2})/(u_{b2}-u_{a2}), & \text{if } u_{a2} < u_2(t) < u_{b2}, \\ 1, & \text{if } u_2(t) \ge u_{b2}, \end{cases} \tag{15}$$

where $u_2(\%)\in[-100, 100]$ and next $u_2\in[-1, 1]$ is the second control input for arm angular position control, the values of the parameters in (15) are [6] $u_{a2}=0.18$, $u_{b2}=1$ and $u_{c2}=0.1538$. The variable $m_3\in[-1, 1]$ is the output of the saturation and dead zone static nonlinearity specific to the third actuator:

$$m_3(t)=\begin{cases}-1, & \text{if } u_3(t)\le -u_{b3},\\ (u_3(t)+u_{c3})/(u_{b3}-u_{c3}), & \text{if } -u_{b3}<u_3(t)<-u_{c3},\\ 0, & \text{if } -u_{c3}\le|u_3(t)|\le u_{a3},\\ (u_3(t)-u_{a3})/(u_{b3}-u_{a3}), & \text{if } u_{a3}<u_3(t)<u_{b3},\\ 1, & \text{if } u_3(t)\ge u_{b3},\end{cases} \tag{16}$$

where $u_3(\%)\in[-100, 100]$ and next $u_3\in[-1, 1]$ is the third control input for payload position control, the values of the parameters in (16) are [6] $u_{a3}=0.1$, $u_{b3}=1$ and $u_{c3}=0.13$.

The nonlinear state-space model of the TCS is [18]

$$\begin{aligned}\dot{x}_1&=x_5,\\ \dot{x}_2&=x_6,\\ \dot{x}_3&=x_7,\\ \dot{x}_4&=x_8,\\ \dot{x}_5&=f_5(\Pi),\\ \dot{x}_6&=f_6(\text{Ш}),\\ \dot{x}_7&=-\frac{1}{T_{\Sigma1}}x_7+\frac{k_{P1}}{T_{\Sigma1}}m_1,\\ \dot{x}_8&=-\frac{1}{T_{\Sigma2}}x_8+\frac{k_{P2}}{T_{\Sigma2}}m_2,\\ \dot{x}_9&=x_{10},\\ \dot{x}_{10}&=f_{10}(\aleph),\\ y_1&=x_3,\\ y_2&=x_4,\\ y_3&=x_9,\end{aligned} \tag{17}$$

in which the expressions of the nonlinear functions f_5, f_6 and f_{10} are

$$\begin{aligned}f_5(\Pi)=f_5(x_1,x_2,x_3,x_5,\ldots,x_{10},m_1,m_2)=\frac{1}{2x_9}(&-4x_5x_{10}+4x_6x_8x_9\cos^2x_1\cos x_2\\ &-x_6^2x_9\sin 2x_1+x_8^2x_9\sin 2x_1\cos^2x_2-2g\sin x_1\cos x_2-4x_7x_8\cos x_1\\ &+2x_3x_8^2\sin x_1\sin x_2+2\frac{x_7}{T_{\Sigma1}}\sin x_1\sin x_2-2\frac{k_{P1}}{T_{\Sigma1}}m_1\sin x_1\sin x_2+4x_8x_{10}\sin x_2\\ &+2\frac{x_3x_8}{T_{\Sigma2}}\cos x_1-2\frac{k_{P2}}{T_{\Sigma2}}x_3m_2\cos x_1-2\frac{x_8x_9}{T_{\Sigma2}}\sin x_2+2\frac{k_{P2}}{T_{\Sigma2}}x_9m_2\sin x_2),\end{aligned} \tag{18}$$

$$
\begin{aligned}
f_6(\text{Ш}) = f_6(x_1, x_2, x_3, x_5, ..., x_{10}, m_1, m_2) = \frac{1}{x_9 \cos x_1}(-2x_6 x_{10} \cos x_1 \\
- 2x_5 x_8 x_9 \cos x_1 \cos x_2 + 2x_5 x_6 x_9 \sin x_1 - g \sin x_2 - 2x_8 x_{10} \sin x_1 \cos x_2 - x_3 x_8^2 \cos x_2 \\
+ x_8^2 x_9 \cos x_1 \cos x_2 \sin x_2 - \frac{x_7}{T_{\Sigma 1}} \cos x_2 + \frac{k_{P1}}{T_{\Sigma 1}} m_1 \cos x_2 + \frac{x_8 x_9}{T_{\Sigma 2}} \sin x_1 \cos x_2 \\
- \frac{k_{P2}}{T_{\Sigma 2}} x_9 m_2 \sin x_1 \cos x_2),
\end{aligned} \tag{19}
$$

$$
\begin{aligned}
f_{10}(\aleph) = f_{10}(x_1, x_2, x_3, x_5, ..., x_{10}, m_1, m_2, m_3) = \frac{1}{1 + \cos x_1 \cos x_2}(-\frac{\mu_L}{m_L} x_{10} + g \\
+ 2x_6 x_{10} \cos x_1 \sin x_2 + 2x_5 x_{10} \sin x_1 \cos x_2 - 2x_5 x_6 x_9 \sin x_1 \sin x_2 \\
+ x_9 f_6(\text{Ш}) \sin x_2 \cos x_1 + x_9 f_5(\prod) \sin x_1 \cos x_2 + x_9 (x_5^2 + x_6^2) \cos x_1 \cos x_2 + \frac{k_{P3} m_3}{m_L}),
\end{aligned} \tag{20}
$$

where, as specified in [6], k_{P1}=0.188 m/s and k_{P2}=0.871 rad/s are gains of the first two DC motors, $T_{\Sigma 1}$=0.1 s and $T_{\Sigma 2}$=0.1 s are time constants for the first two motors in which m_L=0.33 kg is the payload mass, μ_L=1600 kg/s is the viscous coefficient associated with the payload motion, g=9.81 m/s^2 is the gravitational acceleration, k_{P3}=200 kg·m/s^2 is process gain of the third DC motor, and z_c(m) is the z coordinate of the payload.

A part of the model described in Eq. (17) is discretized and next extended by adding the discrete-time integral block for zero stationary control error, and introducing a new state of this integral block [19]:

$$x_{R,k+1} = x_{R,k} + (1/T_i)e_k, \tag{21}$$

where the error is $e_k = r_k - y_k$, the reference input r_k and T_i is the integral time constant (in continuous time). This extended model will have the extended state vector:

$$\mathbf{x}_e = [\mathbf{x}^T \;\; x_R]^T. \tag{22}$$

Using relations (17) and (22) leads to the state vector for cart position control

$$\mathbf{x}_{1e,k} = [x_{3,k} \;\; x_{7,k} \;\; x_{R,k}]^T, \tag{23}$$

for arm angular position control

$$\mathbf{x}_{2e,k} = [x_{4,k} \;\; x_{8,k} \;\; x_{R,k}]^T, \tag{24}$$

and for payload position control

$$\mathbf{x}_{3e,k} = [x_{9,k} \;\; x_{10,k} \;\; x_{R,k}]^T. \tag{25}$$

The gain matrix **K** is considered to have the following structure, where one subscript will be inserted in order to specify one of the three position control systems:

$$\mathbf{K} = [k_1 \quad k_2 \quad k_R]. \tag{26}$$

Three separate single input-single output (SISO) control systems are considered, namely one for each controlled output y_1, y_2 and y_3. Three discrete-time sliding mode controllers discussed in Section 2 are design for each SISO control system. The unified SISO control system structure is illustrated in Fig. 2, where DTSMC specifies the sliding mode controller (position), DTSMC $\in$ {Furuta DTSMC law, Gao DTSMC law, quasi-relay DTSMC law}, $m \in \{1, 2, 3\}$ indicates the number of the controlled output, which is also the number of the control system, and d_m is the disturbance input, not considered in the model (17).

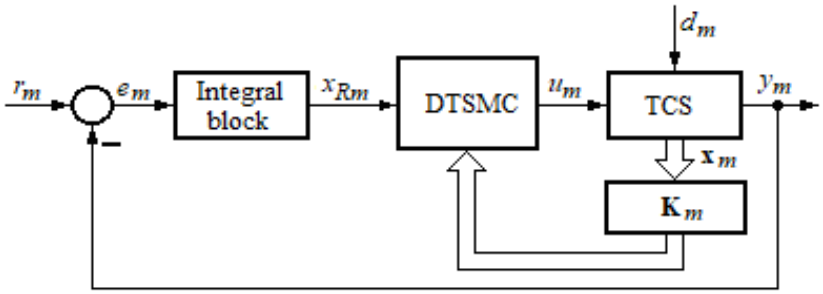

Fig. 2 Unified SISO structure of discrete-time model-based sliding mode control system. The subscript k is omitted for the sake of simplicity.

3.1 Furuta DTSMC law design and implementation

Summarizing the information given in the previous sections, the guidelines to design the Furuta DTSMC law consist of the following steps:

Step F1. Set the values of T_s to account for the requirements of quasi-continuous digital control and T_i, which affects the overshoot and the settling time.

Step F2. Apply Eq. (9) to obtain the expression of the system matrix. Use Eqs. (21) to (25) to express the expression of the extended system matrix (with discrete-time integral block).

Step F3. Choose **K** so that the system described by the matrix obtained at step F2 is stable. Pole placement can be applied in this regard.

Step F4. Apply Eq. (8) to get the upper bound of f_0, and choose a value which is between limits.

These steps are exemplified as follows. For the cart position control system, the sampling period and the integral time constant are chosen as T_s=0.01 s and T_i=0.05 s. The expression of the system matrix is obtained using (9) and (23) [20]

$$\mathbf{A}_{x_1} = \mathbf{A}_{e_1} - \mathbf{B}_{e_1} \cdot (\mathbf{K}_1 \cdot \mathbf{B}_{e_1})^{-1} \cdot \mathbf{K}_1 \cdot (\mathbf{A}_{e_1} - \mathbf{I}) = \begin{bmatrix} 0 & 1 & 0 \\ k_1/k_2 + (2000k_R)/k_2 & 1 - k_1/k_2 & k_R/k_2 \\ -2000 & 0 & 0 \end{bmatrix}. \quad (27)$$

A set of parameters that guarantee the stability of the system with the matrix in Eq. (27) is

$$\mathbf{K}_1 = [3 \quad 0.2 \quad -0.005]. \quad (28)$$

For the upper amplitude of f_0 described in Eq. (8), the matrix $[\mathbf{t}_1\ \mathbf{t}_2\ \mathbf{t}_3]$ is set to $[\mathbf{K}^{-1}\ \mathbf{0}\ \mathbf{0}]$; this gives $0 < f_0 < 15.92$ and the value is set to f_0=1 [20].

The cart position reference input trajectory is chosen to be the same as in [6]. The experimental results obtained for the control system with the controller parameters in Eq. (28) are illustrated in Fig. 3.

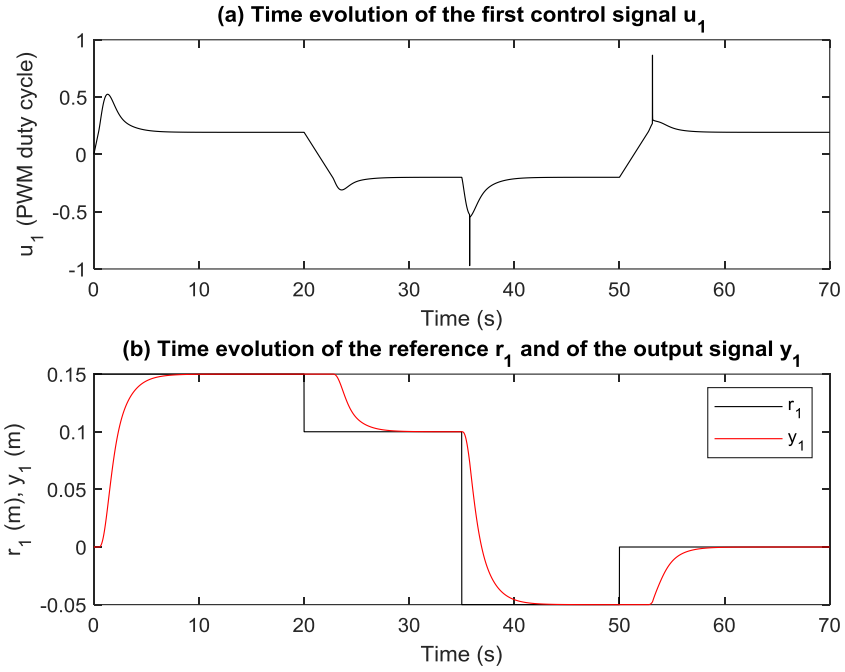

Fig. 3 The results of cart position control system with Furuta DTSMC law: (a) u_1; (b) r_1 (black), y_1 (red).

For the arm angular position control system, the sampling period and the integral time constant are chosen as T_s=0.01 s and T_i=0.012 s. The expression of the system matrix is obtained using Eqs. (9) and (24) [20]

$$\mathbf{A}_{x_2} = \mathbf{A}_{e_2} - \mathbf{B}_{e_2} \cdot (\mathbf{K}_2 \cdot \mathbf{B}_{e_2})^{-1} \cdot \mathbf{K}_2 \cdot (\mathbf{A}_{e_2} - \mathbf{I}) = \begin{bmatrix} 0 & 1 & 0 \\ k_1/k_2 + (25000k_R)/3k_2 & 1 - k_1/k_2 & k_R/k_2 \\ -25000/3 & 0 & 0 \end{bmatrix}. \quad (29)$$

A set of parameters that guarantee the stability of the system with the matrix in (29) is

$$\mathbf{K}_2 = [3.15 \quad 0.2 \quad -0.0002]. \quad (30)$$

For the upper amplitude of f_0 described in Eq. (8), the matrix $[\mathbf{t}_1\ \mathbf{t}_2\ \mathbf{t}_3]$ is set to $[\mathbf{K}^{-1}\ \mathbf{0}\ \mathbf{0}]$; this gives $0 < f_0 < 3.63$ and the value is set to f_0=3 [20].

The arm angular position reference input trajectory is chosen to be the same as in [6]. The experimental results obtained for the control system with the controller parameters in Eq. (30) are illustrated in Fig. 4.

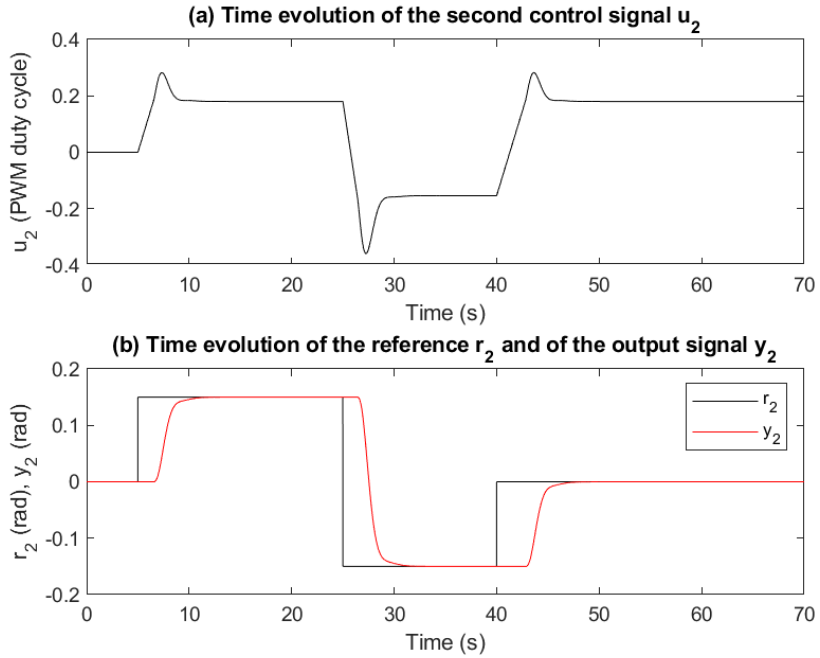

Fig. 4 The results of arm angular position control system with Furuta DTSMC law: (a) u_2; (b) r_2 (black), y_2 (red).

For the payload position control system, the sampling period and the integral time constant are chosen as T_s=0.01 s and T_i=0.0001 s. The expression of the system matrix is obtained using Eqs. (9) and (25) [20]

$$\mathbf{A}_{x_3} = \mathbf{A}_{e_3} - \mathbf{B}_{e_3} \cdot (\mathbf{K}_3 \cdot \mathbf{B}_{e_3})^{-1} \cdot \mathbf{K}_3 \cdot (\mathbf{A}_{e_3} - \mathbf{I}) = \begin{bmatrix} 0 & 1 & 0 \\ k_1/k_2 + (1000000k_R)/k_2 & 1 - k_1/k_2 & k_R/k_2 \\ -1000000 & 0 & 0 \end{bmatrix}. \quad (31)$$

A set of parameters that guarantee the stability of the system with the matrix in (29) is

$$\mathbf{K}_3 = [59.0909 \quad 0.011 \quad 0]. \quad (32)$$

For the upper amplitude of f_0 described in (8), the matrix $[\mathbf{t}_1\ \mathbf{t}_2\ \mathbf{t}_3]$ is set to $[\mathbf{K}^{-1}\ \ \mathbf{0}\ \ \mathbf{0}]$; this gives $0 < f_0 < 107.43$ and the value is set to f_0=106 [20].

The payload position reference input trajectory is chosen to be the same as in [6]. The experimental results obtained for the control system with the controller parameters in Eq. (32) are illustrated in Fig. 5.

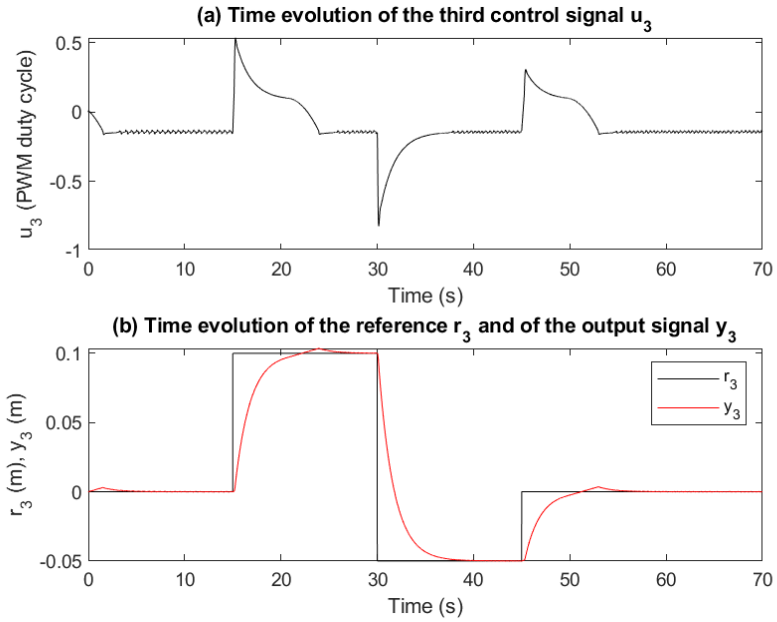

Fig. 5 The results of payload position control system with Furuta DTSMC law: (a) u_3; (b) r_3 (black), y_3 (red).

3.2 Gao DTSMC law design and implementation

Summarizing the information given in the previous sections, the guidelines to design the Gao DTSMC law consist of the following steps:

Step G1. This step is identical to step F1.

Step G2. This step is identical to step F2.

Step G3. This step is identical to step F3.

Step G4. Set $q>0$ to fulfill $q \cdot T_s \in (0,1)$, and $\varepsilon>0$.

These steps are exemplified as follows. For the cart position control system, the sampling period and the integral time constant are chosen as T_s=0.01 s and T_i=0.2 s. The expression of the system matrix specific to the Furuta DTSMC law results from Eqs. (9) and (23) [20]

$$\mathbf{A}_{x_1} = \mathbf{A}_{e_1} - \mathbf{B}_{e_1} \cdot (\mathbf{K}_1 \cdot \mathbf{B}_{e_1})^{-1} \cdot \mathbf{K}_1 \cdot (\mathbf{A}_{e_1} - \mathbf{I}) = \begin{bmatrix} 0 & 1 & 0 \\ k_1/k_2 + (500k_R)/k_2 & 1 - k_1/k_2 & k_R/k_2 \\ -500 & 0 & 0 \end{bmatrix}. \quad (33)$$

A set of parameters that guarantee the stability of the system with the matrix in (33) is

$$\mathbf{K}_1 = [0.825 \quad 0.4 \quad -0.0011]. \quad (34)$$

The other parameters of the control law were set as q=99 such that $q \cdot T_s \in (0,1)$ and ε=200 [20].

Using the same reference input trajectory as in Section 3.1 and [6], the experimental results obtained for the control system with the controller parameters in Eq. (34) are given in Fig. 6.

For the arm angular position control system, the sampling period and the integral time constant are chosen as T_s=0.01 s and T_i=0.2 s. The expression of the system matrix specific to the Furuta DTSMC law results from Eqs. (9) and (24) [20]

$$\mathbf{A}_{x_2} = \mathbf{A}_{e_2} - \mathbf{B}_{e_2} \cdot (\mathbf{K}_2 \cdot \mathbf{B}_{e_2})^{-1} \cdot \mathbf{K}_2 \cdot (\mathbf{A}_{e_2} - \mathbf{I}) = \begin{bmatrix} 0 & 1 & 0 \\ k_1/k_2 + (500k_R)/k_2 & 1 - k_1/k_2 & k_R/k_2 \\ -500 & 0 & 0 \end{bmatrix}. \quad (35)$$

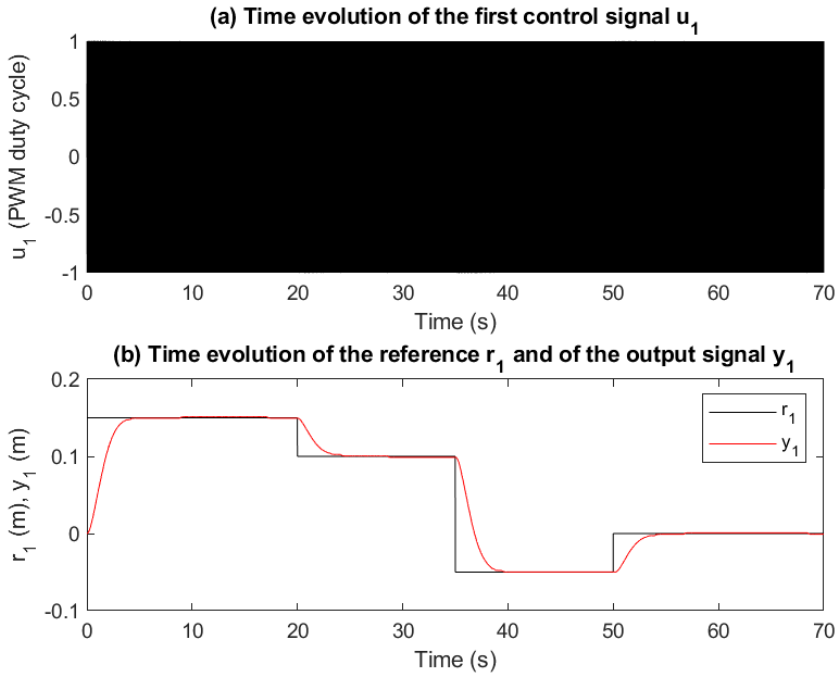

Fig. 6 The results of cart position control system with Gao DTSMC law: (a) u_1; (b) r_1 (black), y_1 (red).

A set of parameters that guarantee the stability of the system with the matrix in Eq. (35) is

$$\mathbf{K}_2 = [0.825 \quad 0.4 \quad -0.0011]. \quad (36)$$

The other parameters of the control law were set as q=99 such that $q \cdot T_s \in (0,1)$ and ε=500 [20].

Using the same reference input trajectory as in Section 3.2 and [6], the experimental results obtained for the control system with the controller parameters in Eq. (36) are given in Fig. 7.

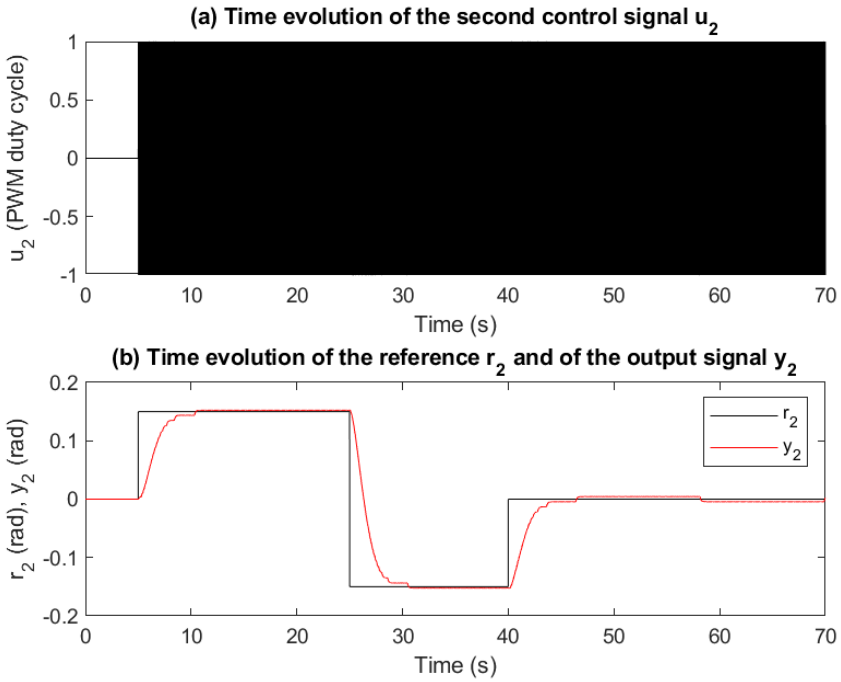

Fig. 7 The results of arm angular position control system with Gao DTSMC law: (a) u_2; (b) r_2 (black), y_2 (red).

For the payload position control system, the sampling period and the integral time constant are chosen as T_s=0.01 s and T_i=0.0025 s. The expression of the system matrix specific to the Furuta DTSMC law results from Eqs. (9) and (25) [20]

$$\begin{aligned}\mathbf{A}_{x_3} &= \mathbf{A}_{e_3} - \mathbf{B}_{e_3}\cdot(\mathbf{K}_3\cdot\mathbf{B}_{e_3})^{-1}\cdot\mathbf{K}_3\cdot(\mathbf{A}_{e_3}-\mathbf{I}) \\ &= \begin{bmatrix} 0 & 1 & 0 \\ k_1/k_2 + (6871947673599999k_R)/17179869184k_2 & 1-k_1/k_2 & k_R/k_2 \\ -6871947673599999/17179869184 & 0 & 0 \end{bmatrix}.\end{aligned} \tag{37}$$

A set of parameters that guarantee the stability of the system with the matrix in Eq. (37) is

$$\mathbf{K}_3 = [61.92 \quad 0.0130 \quad 0]. \tag{38}$$

The other parameters of the control law were set as q=99 such that $q\cdot T_s \in (0,1)$ and ε=300 [20].

Using the same reference input trajectory as in Section 3.3 and [6], the experimental results obtained for the control system with the controller parameters in Eq. (38) are given in Fig. 8.

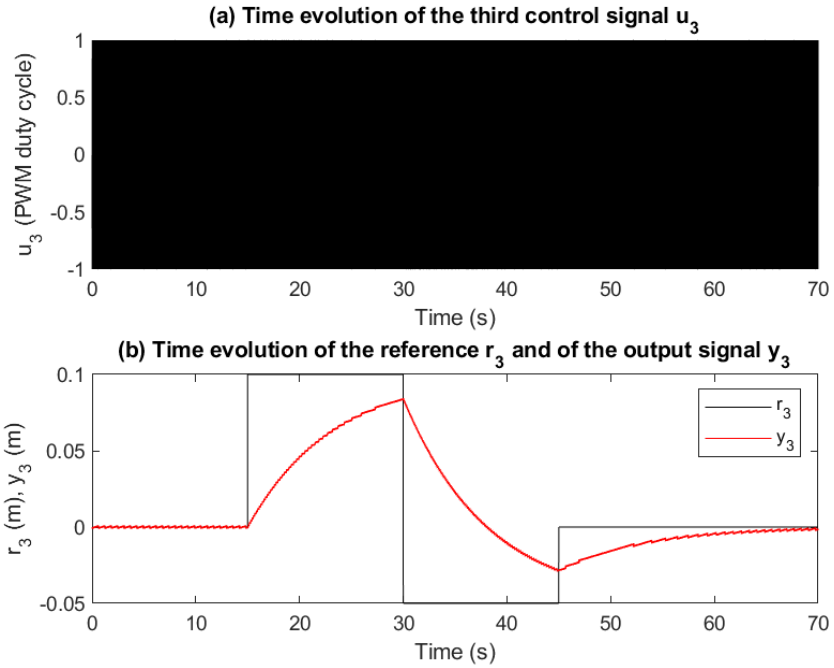

Fig. 8 The results of payload position control system with Gao DTSMC law: (a) u_3; (b) r_3 (black), y_3 (red).

3.3 Quasi-relay DTSMC law design and implementation

Summarizing the information given in the previous sections, the guidelines to design the quasi-relay DTSMC law consist of the following steps:

Step M1. This step is identical to step F1.

Step M2. This step is identical to step F2.

Step M3. This step is identical to step F3.

Step M4. Set the values of the parameters $\omega_i>1$.

These steps are exemplified as follows. For the cart position control system, the sampling period and the integral time constant are chosen as T_s=0.01 s and T_i=0.25 s. The expression of the system matrix specific to the Furuta DTSMC law results from Eqs. (9) and (23) [20]

$$\mathbf{A}_{x_1}=\mathbf{A}_{e_1}-\mathbf{B}_{e_1}\cdot(\mathbf{K}_1\cdot\mathbf{B}_{e_1})^{-1}\cdot\mathbf{K}_1\cdot(\mathbf{A}_{e_1}-\mathbf{I})=\begin{bmatrix}0 & 1 & 0\\ k_1/k_2+(500k_R)/k_2 & 1-k_1/k_2 & k_R/k_2\\ -500 & 0 & 0\end{bmatrix}. \quad (39)$$

A set of parameters that guarantee the stability of the system with the matrix in (39) is

$$\mathbf{K}_1=[0.9 \quad 0.4 \quad -0.001]. \quad (40)$$

The other parameters of the control law were set as $\boldsymbol{\omega}$=[3 1 3] [20].

Using the same reference input trajectory as in Section 3.1 and [6], the experimental results obtained for the control system with the controller parameters in Eq. (40) are illustrated in Fig. 9.

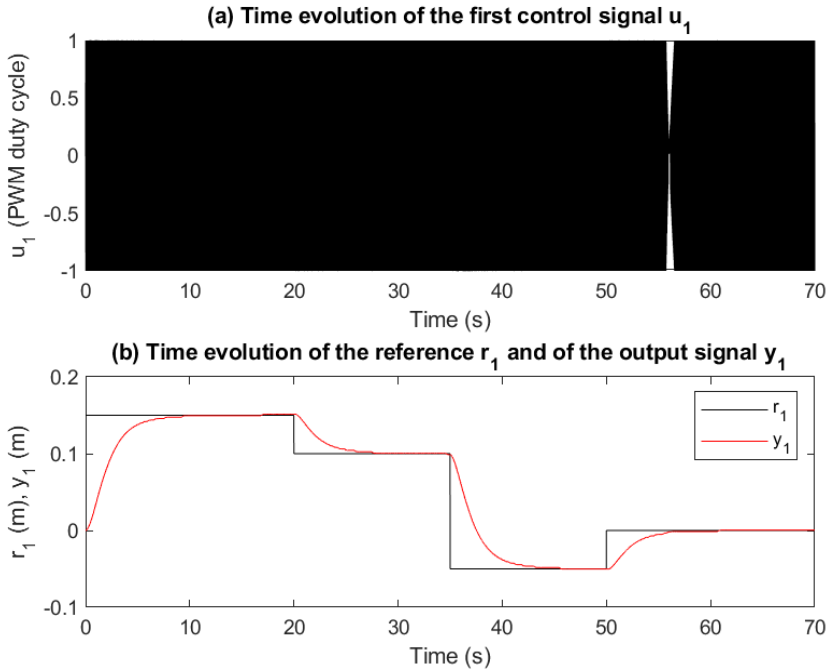

Fig. 9 The results of cart position control system with quasi-relay DTSMC law: (a) u_1; (b) r_1 (black), y_1 (red).

For the arm angular position control system, the sampling period and the integral time constant are chosen as T_s=0.01 s and T_i=0.25 s. The expression of the system matrix specific to the Furuta DTSMC law results from Eqs. (9) and (24) [20]

$$\mathbf{A}_{x_2} = \mathbf{A}_{e_2} - \mathbf{B}_{e_2} \cdot (\mathbf{K}_2 \cdot \mathbf{B}_{e_2})^{-1} \cdot \mathbf{K}_2 \cdot (\mathbf{A}_{e_2} - \mathbf{I}) = \begin{bmatrix} 0 & 1 & 0 \\ k_1/k_2 + (400k_R)/k_2 & 1 - k_1/k_2 & k_R/k_2 \\ -400 & 0 & 0 \end{bmatrix}. \quad (41)$$

A set of parameters that guarantee the stability of the system with the matrix in Eq. (41) is

$$\mathbf{K}_2 = [0.83 \quad 0.3 \quad -0.0011]. \quad (42)$$

The other parameters of the control law were set as $\boldsymbol{\omega}$=[3 1 3] [20].

Using the same reference input trajectory as in Section 3.2 and [6], the experimental results obtained for the control system with the controller parameters in Eq. (42) are illustrated in Fig. 10.

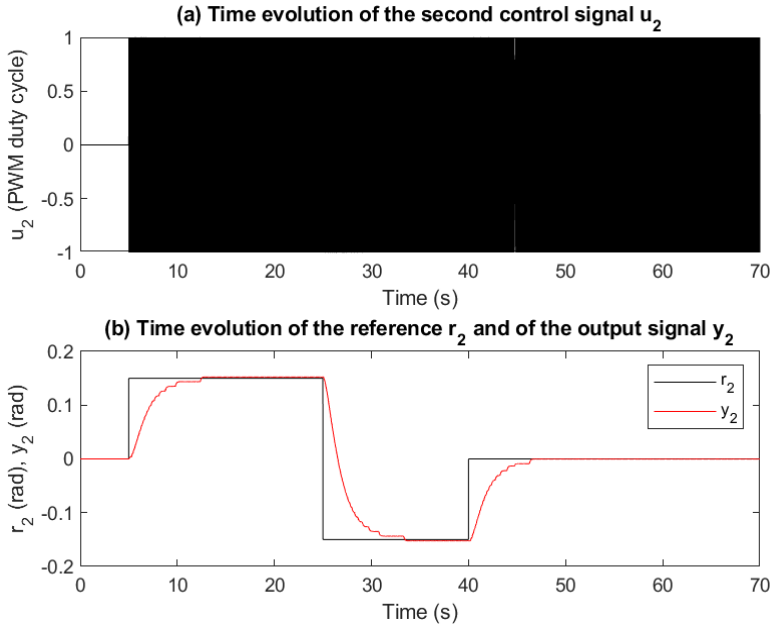

Fig. 10 The results of arm angular position control system with quasi-relay DTSMC law: (a) u_2; (b) r_2 (black), y_2 (red).

For the payload position control system, the sampling period and the integral time constant are chosen as T_s=0.01 s and T_i=0.003 s. The expression of the system matrix specific to the Furuta DTSMC law results from Eqs. (9) and (25) [20]

$$\begin{aligned}\mathbf{A}_{x_3} &= \mathbf{A}_{e_3} - \mathbf{B}_{e_3} \cdot (\mathbf{K}_3 \cdot \mathbf{B}_{e_3})^{-1} \cdot \mathbf{K}_3 \cdot (\mathbf{A}_{e_3} - \mathbf{I}) \\ &= \begin{bmatrix} 0 & 1 & 0 \\ k_1/k_2 + (100000k_R)/3k_2 & 1 - k_1/k_2 & k_R/k_2 \\ -100000/3 & 0 & 0 \end{bmatrix}.\end{aligned} \tag{43}$$

A set of parameters that guarantee the stability of the system with the matrix in (43) is

$$\mathbf{K}_3 = [7 \quad 0.1 \quad -0.0003]. \tag{44}$$

The other parameters of the control law were set as $\boldsymbol{\omega}$=[50 25 10] [20].

Using the same reference input trajectory as in Section 3.3 and [6], the experimental results obtained for the control system with the controller parameters in Eq. (44) are illustrated in Fig. 11.

For a fair comparison of the three DTSMC laws, it is accepted that the allowable tolerance zone of the controlled output is of ± 2 % y_{st}, where y_{st} is the steady-state value of the controlled output. This is reflected in the measurement of the values of the overshoot and the settling time.

The performance indices overshoot, settling time and stationary control error (or steady-state value of control error) are considered in the comparison of the control

systems with the three DTSMC laws designed in this paper. The values of these performance indices are synthesized in Table 1, Table 2 and Table 3, obtained after three test runs for all three control systems with DTSMC laws with extended state vectors defined in Eqs. (23), (24) and (25), respectively. The test runs are composed by three step signals, three step signals, and four step signals, respectively.

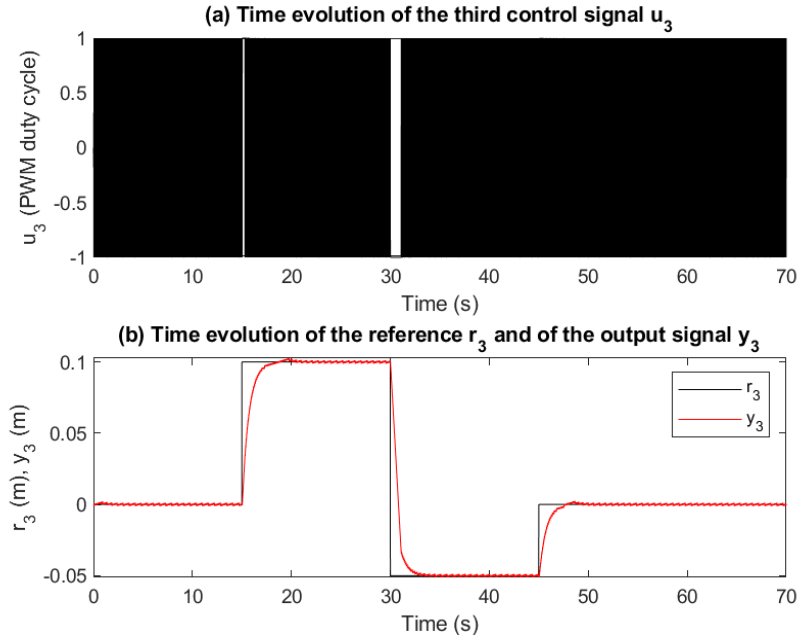

Fig. 11 The results of payload position control system with quasi-relay DTSMC law: (a) u_3; (b) r_3 (black), y_3 (red).

Table 1 Overshoot (%)

Test run	Step	Quasi-relay	Furuta	Gao
Cart position	1	0	0	0
	2	0	0	0
	3	0	0	0
	4	0	0	0
	$\overline{X}$	0	0	0
Arm angular position	1	0	0	0
	2	0	0	0
	3	0	0	0
	$\overline{X}$	0	0	0
Payload position	1	2.7	3.5	–
	2	0	0	–
	3	5	0	0
	$\overline{X}$	2.6	1.2	–

$\overline{X}$ – average value of the steps which compose the reference signal

Table 2 Settling time (s)

Test run	Step	Quasi-relay	Furuta	Gao
Cart position	1	7.55	6.5	4.2
	2	6.2	7	3.5
	3	8.2	6	4.4
	4	6	8.6	4.5
	$\overline{X}$	6.987	7.025	4.15
Arm angular position	1	7.4	5.5	5.4
	2	8.4	6	5.5
	3	6.6	7.4	6.5
	$\overline{X}$	7.467	6.3	5.8
Payload position	1	4.8	9.6	–
	2	2.8	7	–
	3	5	9.6	16
	$\overline{X}$	4.2	8.733	–

$\overline{X}$ – average value of the steps which compose the reference signal

Table 3 Stationary control error (%)

Cart position	Step	Quasi-relay	Furuta	Gao
	1	1	0	0
Arm angular position	2	1.2	0.1	1.2
	3	0.6	0	0.1
	4	1.5	0	0
	$\overline{X}$	1	0	0.3
	1	1.6	0	1.6
Payload position	2	0	0	0.8
	3	0.2	0	0
	$\overline{X}$	0.6	0	0.8
	1	0.4	0.1	–
	2	0.3	0	–
	3	0	0	5.2
	$\overline{X}$	0.2	0	–

$\overline{X}$ – average value of the steps which compose the reference signal

Analyzing the values for the overshoot in Table 1 reveals the fact that the smallest average value is exhibited by the Furuta DTSMC law. In Table 2, the smallest average value of the settling time is obtained by the quasi-relay DTSMC law. Table 3 shows that the Furuta DTSMC law exhibits the smallest average value as far as the stationary control error is concerned.

In conclusion, having in mind all three performance indices discussed here, the best overall performance is ensured by the Furuta DTSMC law, the second best one is Gao DTSMC low and on the third place is Quasi-relay DTSCM low. Nevertheless, the Furuta DTSMC law leads to the smallest number of switching of the control inputs, thus the efforts at the level of actuators (namely, the power electronics part that produces PWM). However, the conclusions of the comparison can be different if other nonlinear processes are subjected to sliding mode control, in various fields, including decision-making [21], man-

computer symbiosis [22], 3D printing objects [23], specific structures of fuzzy systems [24], [25] including those focused on fuzzy control [26], [27], evolving controllers [28] and fuzzy cognitive maps [29], VANETs [30], quantum computing [31], and telesurgical applications [32].

Disturbance inputs were not considered (although the role of a part of possible disturbances is highlighted in Fig. 2) because the integral block described in [21] ensures the disturbance rejections for certain types of disturbances. It is not guaranteed that the ranking of the sliding mode controllers will be kept after rejecting the disturbances.

4. CONCLUSIONS

This paper proposed the discrete-time model-based sliding mode control of tower crane systems. Three popular control discrete-time control laws were considered and compared systematically on the basis of three performance indices obtained after measurements in a specific dynamic regime applied to the laboratory equipment.

The Furuta law was applied to all three control laws to design the gain matrix **K** in the conditions of the application of the equivalent control method [2]. However, the control laws are different in terms of different ways to carry out the switching that modifies the control system structures making them belong to the general class of variable structure systems. The parameters involved in switching are also different. This flexibility is an advantage of the control laws designed and implemented in this paper and also confirms the degrees of freedom offered by sliding mode control, also showing certain robustness.

One of the main shortcomings of these control laws is the heuristics in the design of the controllers. Another shortcoming is the need for certain initial information on the process model. Future research will be focused on mitigating these shortcomings. First, the optimal tuning of the free parameters of the sliding mode controllers will be targeted. Second, the design of data-driven sliding mode controllers will be carried out starting with [6] and compared to model-based sliding mode controllers. Direct relations that involve controller tuning parameters and control system performance indices with respect to both reference and disturbance inputs will be attempted to be derived in all controller designs.

Acknowledgement: *The research reported in this paper was supported by a grant of the Romanian Ministry of Education and Research, CNCS - UEFISCDI, project number PN-III-P4-ID-PCE-2020-0269, within PNCDI III.*

REFERENCES

1. Emelyanov, S.V., 1967, *Variable Structure Control Systems*. Nauka, Moscow.
2. Utkin, V.I., 1977, *Variable structure systems with sliding modes*, IEEE Transactions on Automatic Control, 22(2), pp. 212-222.
3. Yu, X.-H., Kaynak, O., 2009, *Sliding-mode control with soft computing: A survey*, IEEE Transactions on Industrial Electronics, 56(9), pp. 3275-3285.
4. Young, K.D., Utkin, V.I., Ozguner, U., 1999, *A control engineer's guide to sliding mode control*, IEEE Transactions on Control Systems Technology, 7(3), pp. 328-342.

5. Aboserre, L.T., El-Badawy, A.A., 2020, *Robust integral sliding mode control of tower cranes*, Journal of Vibration and Control, 27(9-10), pp. 1171-1183.
6. Precup, R.-E., Roman, R.-C., Safaei, A., 2021, *Data-Driven Model-Free Controllers*, 1st edition. CRC Press, Taylor & Francis, Boca Raton, FL.
7. Xi, Z., Hesketh, T., 2010, *Discrete time integral sliding mode control for overhead crane with uncertainties*, IET Control Theory & Applications, 4(10), pp. 2071-2081.
8. Qian, D.-W., Yi, J.-Q., 2013, *Design of combining sliding mode controller for overhead crane systems*, International Journal of Control and Automation, 6(1), pp. 132-140.
9. Bartolini, G., Orani, N., Pisano, A., Usai, E., 2000, *Load swing damping in overhead cranes by sliding mode technique*, Proc. 39th IEEE Conference on Decision and Control, Sydney, NSW, Australia, vol. 2, pp. 1697–1702.
10. Lee, L.-H., Huang, C.-H., Ku, S.-C., Yang, Z.-H., Chang, C.-Y., 2014, *Efficient visual feedback method to control a three-dimensional overhead crane*, IEEE Transactions on Industrial Electronics, 61(8), pp. 4073-4083.
11. Sun, N., Fang, Y.-C., Chen, H., Lu, B., Fu, Y.-M., 2016, *Slew/translation positioning and swing suppression for 4-dof tower cranes with parametric uncertainties: Design and hardware experimentation*, IEEE Transactions on Industrial Electronics, 63(10), pp. 6407-6418.
12. Le, T.A., Dang, V.-H, Ko, D.H., An, T.N., Lee, S.-G., 2013, *Nonlinear controls of a rotating tower crane in conjunction with trolley motion*, Proceedings of the Institution of Mechanical Engineers, Part I: Journal of Systems and Control Engineering, 227(5), pp. 451–460.
13. Aboserre, L.T., El-Badawy, A.A., 2021, *Robust integral sliding mode control of tower cranes*, Journal of Vibration and Control, 27(9-10), pp. 1171-1183.
14. Furuta, K., 1990, *Sliding mode control of a discrete system*, Systems & Control Letters, 14(2), pp. 145-152.
15. Gao, W.-B., Wang, Y.-F., Homaifa, A., 1995, *Discrete-time variable structure control systems*, IEEE Transactions on Industrial Electronics, 42(2), pp. 117-122.
16. Milosavljević, Č., 1985, *General conditions for the existence of a quasisliding mode on the switching hyperplane in discrete variable structure systems*, Automation and Remote Control, 46(3), pp. 307-314.
17. Spasić, M.D., 2019, *Model predictive control based on sliding mode control*, Ph.D. thesis, University of Niš, Niš, Serbia.
18. Inteco, 2012, *Tower Crane, User's Manual*, Inteco Ltd, Krakow.
19. Buehler, H., 1986, *Reglage par mode de glissement*. Presses Polytechniques Romandes, Lausanne.
20. Borlea, A.-I., 2022, *Sliding mode controllers. Validation on a laboratory equipment* (in Romanian), M.Sc. thesis, Politehnica University of Timisoara, Timisoara, Romania.
21. Božanić, D., Tešić, D., Marinković, D., Milić, A., 2021, *Modeling of neuro-fuzzy system as a support in decision-making processes*, Reports in Mechanical Engineering, 2(1), pp. 222-234.
22. Filip, F.G., 2021, *Automation and computers and their contribution to human well-being and resilience*, Studies in Informatics and Control, 30(4), pp. 5-18.
23. Milićević, I., Popović, M., Dučić, N., Vujičić, V., Stepanić, P., Marinković, D., Ćojbašić, Ž., 2022, *Improving the mechanical characteristics of the 3D printing objects using hybrid machine learning approach*, Facta Universitatis-Series Mechanical Engineering, doi: 10.22190/FUME220429036M.
24. Yapici Pehlivan, N., Turksen, I.B., 2021, *A novel multiplicative fuzzy regression function with a multiplicative fuzzy clustering algorithm*, Romanian Journal of Information Science and Technology, 24(1), pp. 79-98.
25. Kwak, C.-J., Ri, K.-C., Kwak, S.-I., Kim, K.-J., Ryu, U.-S., Kwon, O.-C., Kim, N.-H., 2021, *Fuzzy modus ponens and tollens based on moving distance in SISO fuzzy system*, Romanian Journal of Information Science and Technology, 24(3), pp. 257-283.
26. Precup, R.-E., Preitl, S., Balas, M., Balas, V., 2004, *Fuzzy controllers for tire slip control in anti-lock braking systems*, Proc. 2004 IEEE International Conference on Fuzzy Systems, Budapest, Hungary, vol. 3, pp. 1317-1322.
27. Preitl, Z., Precup, R.-E., Tar, J.K., Takács, M., 2006, *Use of multi-parametric quadratic programming in fuzzy control systems*, Acta Polytechnica Hungarica, 3(3), pp. 29-43.
28. Škrjanc, I., Blažič, S., Angelov, P., 2014, *Robust evolving cloud-based PID control adjusted by gradient learning method*, Proc. 2014 IEEE Conference on Evolving and Adaptive Intelligent Systems, Linz, Austria, pp. 1-6.
29. Vaščák, J., Hvizdoš, J., Puheim, M., 2016, *Agent-based cloud computing systems for traffic management*, Proc. 2016 International Conference on Intelligent Networking and Collaborative Systems, Ostrava, Czech Republic, pp. 73-79.

30. Boucetta, S.I., Johanyák, Z.C., Pokorádi, L.K., 2017, *Survey on software defined VANETs*, Gradus, 4(1), pp. 272-283.
31. Osaba, E., Villar-Rodriguez, E., Oregi, I., Moreno-Fernandez-de-Leceta, A., 2021, *Hybrid quantum computing-tabu search algorithm for partitioning problems: preliminary study on the traveling salesman problem*, Proc. 2021 IEEE Congress on Evolutionary Computation, Kraków, Poland, pp. 351-358.
32. Precup, R.-E., Haidegger, T., Preitl, S., Benyó, B., Paul, A.S., Kovács, L., 2012, *Fuzzy control solution for telesurgical applications*, Applied and Computational Mathematics, 11(3), pp. 378-397.